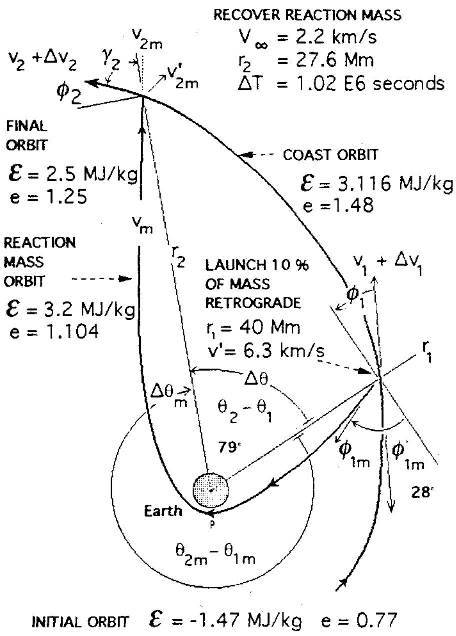

Fig. 2 Point case of net Δv with two-way EML.

that the masses ejected are "smart" in the sense that they have enough onboard computation and propulsion capability to effect rendezvous at high velocity. Forward proposed that incoming masses dock with a cradle that had been accelerated along the launcher up to the incoming velocity.[3] Alternatively, a magnet-equipped spacecraft could simply "land" on its EML "rails" roughly analogous to aircraft carrier landings (the velocities are an order of magnitude higher, but electronic reactions are several orders of magnitude higher than human reactions, and the platform is stable). After "landing," the spacecraft would be, essentially, a high-speed maglev rail coach.

From certain orbits, a two-way EML-equipped vehicle could generate significant outward velocity without loss of reaction mass—effectively using the planet as its reaction mass. Figure 2 is a point example of this.[6] The general bounds on this concept need to be defined, but one can imagine that, in addition to L1 stationkeeping, satellites could be pushed away from planets, or planets away from the sun, without loss of reaction mass—given time and an energy source sufficient to make up for the change in potential energy and any inefficiencies.

Forward[3] briefly addressed the possibility of levitation. This might be done by rotating the line of apsides at the periapsis of the orbit of the reaction mass to make the reaction mass reintercept a stationary EML. Around planets with atmospheres, this might also be accomplished by using negative lift near periapsis. In addition, gas might be collected and brought back out to the levitating EML, provided the initial velocity was high enough.

Acknowledgments

This work was supported by the author. The interest and encouragement of Robert L. Forward are gratefully acknowledged.

References

[1]Clarke, A. C., "Electromagnetic Launching as a Major Contribution to Space Flight," *Journal of the British Interplanetary Society*, Vol. 9, No. 6, 1950, pp. 261–267.

[2]O'Neill, G. K., *The High Frontier*, Bantam Books, New York, 1978.

[3]Forward, R. L., Conley, R., Stanek, C., and Ramsey, W., "The Cable Catapult; Putting It There and Keeping It There," AIAA Paper 92-3077, July 1992.

[4]Verne, J., *Autour de la Lune*, Hetzel, Paris, 1865.

[5]Bate, R. R., Mueller, D., and White, J., *Fundamentals of Astrodynamics*, Dover, New York, 1971, p. 188.

[6]Nordley, G. D., "Two-Way EML Propulsion," *NASA Office of Advanced Concepts and Technology 4th Advanced Propulsion Workshop*, edited by R. H. Frisbee, 1994, pp. 102–105 (JPL D-10673).

Simple Estimation Algorithm for Performance-Seeking Controllers

Martín D. España*
National Research Council,
NASA Dryden Flight Research Center,
Edwards, California 93523

Introduction

THE performance-seeking-control algorithm (PSC) is designed to continuously optimize the performance of a propulsion system. The optimization is based on a steady-state model, called the optimization model, that includes the inlet, engine, and nozzle. To account for significant deviations with respect to nominal conditions experienced by the engine during its life span (engine deterioration), or for engine-to-engine manufacturing variability, the optimization model includes a set of adjustable parameters called the engine deviation parameters (EDPs), denoted as[1–4]

$$\boldsymbol{\eta}^T: = [\text{DEHPT DELPT DWHPC DWFAN AAHT}] \quad (1)$$

where

AAHT	=	area adder high-pressure turbine deviation parameter, in.^{2}
DEHPT	=	high-pressure turbine efficiency deviation parameter, %
DELPT	=	low-pressure turbine efficiency deviation parameter, %
DWFAN	=	fan airflow component deviation parameter, lb/s
DWHPC	=	high-pressure compressor airflow deviation parameter, lb/s

By definition, for the nominal engine, $\boldsymbol{\eta} = 0$. $\boldsymbol{\eta}$ is currently estimated in flight using a Kalman filter based on a dynamic model of the engine called the estimation model.

Optimization Model of the PSC Algorithm

The optimization model of the PSC algorithm is a simplified steady-state model of the propulsion system called the compact propulsion system model (CPSM). Part of it is the engine's steady-state variable model (SSVM), which consists of a piecewise linearization of the steady-state aerothermodynamic equations of the engine around a set of base points covering the power-setting range of the reference flight condition (i.e., standard day, Mach 0.9, and altitude 30,000 ft). Each of the linear models, valid in a neighborhood of a base point, is described by the equation:

$$\boldsymbol{y} = G_y \boldsymbol{u} + H_y \boldsymbol{\eta} \quad (2)$$

Received July 19, 1993; revision received Feb. 26, 1994; accepted for publication March 28, 1994. This paper is declared a work of the U.S. Government and is not subject to copyright protection in the United States.

*Propulsion Branch, P.O. Box 273, M/S 4840A. Member AIAA.

relating $\boldsymbol{\eta}$ with vectors $\boldsymbol{u} \in \mathbb{R}^6$ and $\boldsymbol{y} \in \mathbb{R}^5$ which are, respectively, small (local) deviations of the (engine) input vector, and of the measurable output vector. Matrices $G_y \in \mathbb{R}^{5\times6}$ and $H_y \in \mathbb{R}^{5\times5}$ are calculated a priori for each local model, by numeric linearization using a high fidelity model called the state of the art propulsion program (SOAPP).[1] The matrices are updated in flight, using as indices the measures of 1) the total pressure at the inlet of the high pressure turbine PT4, and 2) the total pressure at the inlet of the afterburner PT6. More details on this model can be found in Ref. 2.

Estimation Algorithm of the PSC Current Design

The vector $\boldsymbol{\eta}$ is currently estimated using a Kalman filter (KF) based on a set of local engine's linear dynamic models (Refs. 1 and 4) represented as

$$\dot{\boldsymbol{x}} = A\boldsymbol{x} + B\boldsymbol{u} + L\boldsymbol{\eta} + \boldsymbol{\omega}_x \tag{3a}$$

$$\dot{\boldsymbol{\eta}} = \boldsymbol{\omega}_\eta \tag{3b}$$

$$\boldsymbol{y} = C\boldsymbol{x} + D\boldsymbol{u} + M\boldsymbol{\eta} + \boldsymbol{\rho} \tag{3c}$$

where $\boldsymbol{x} \in \mathbb{R}^3$ is a reduced-order engine state; $\boldsymbol{u}$ and $\boldsymbol{y}$ are defined as in Eq. (2); $\boldsymbol{\omega}_\eta$, $\boldsymbol{\omega}_x$, and $\boldsymbol{\rho}$ are zero-mean white noises with positive definite covariance matrices, respectively, Q_η, Q_x, and R. Model (2) is the steady-state version of model (3); however, the matrices A to M, also calculated by numeric linearization using the SOAPP, are determined for a set of 49 base points (indexed only by PT4), which are different from those used for Eq. (2).

Under certain observability conditions of model (3), discussed in Ref. 5, η and the state vector $\boldsymbol{x}$ can be estimated using the steady-state KF[6,7] determined from

$$\begin{bmatrix} \dot{\hat{x}} \\ \dot{\hat{\boldsymbol{\eta}}} \end{bmatrix} = F\begin{bmatrix} \hat{x} \\ \hat{\boldsymbol{\eta}} \end{bmatrix} + G\boldsymbol{u} + K\left(\boldsymbol{y} - H\begin{bmatrix} \hat{x} \\ \hat{\boldsymbol{\eta}} \end{bmatrix}\right) \tag{4}$$

$$F := \begin{bmatrix} A & L \\ 0 & 0 \end{bmatrix}, \qquad G := \begin{bmatrix} B \\ 0 \end{bmatrix}, \qquad H := [C \,\vdots\, M]$$
$$K := \begin{bmatrix} K_x \\ K_\eta \end{bmatrix} = PH^TR^{-1}, \qquad Q := \begin{bmatrix} Q_x & 0 \\ 0 & Q_\eta \end{bmatrix} \tag{5}$$

$$FP + PF^T + Q - PH^TR^{-1}HP = 0 \tag{6}$$

The covariance matrix R is estimated from sample statistics of the measurements of the outputs variables, whereas the entries of the submatrices Q_x and Q_η are used as "tuning parameters," empirically adjusted (by simulation) so as to obtain a good compromise between time response and noise rejection for each of the 49 base points used to define the model (3). The design gives as a result 49 matrices $K \in \mathbb{R}^{8\times5}$ that are stored together with the matrices A to M. All the Kalman filter matrices are recovered in flight using PT4 as the index variable.

Because of the artificial introduction of the matrix Q_η, no claim can be made concerning the optimality of the resulting filter. Furthermore, as can be seen from Eqs. (4–6), the filter's eigenvalues (those of the matrix $F - KH$) are not directly linked to the tuning parameters (entries of the matrix Q_η). This complicates the tuning of the filter's dynamic response, which can only be done after extensive simulations.

Estimation of the EDPs with a Luenberger Observer Based on the SSVM

Given the local nature of the models involved, in practice, the estimation is deactivated during engine transients (this is consistent with the objectives of the PSC algorithm, which only attempts to optimize the engine in steady state). Consequently, the data fed into the Kalman filter is mainly acquired during steady state. These facts open up the question of whether a dynamic model, different from the (steady-state) optimization model, is justified for the PSC estimation algorithm. As an alternative, we consider the following $\boldsymbol{\eta}$ estimator based on the SSVM, called the steady-state model-based Luenberger observer (SSMLO):

$$\dot{\hat{\boldsymbol{\eta}}} = -K_0(\hat{\boldsymbol{y}} - \boldsymbol{y}) \tag{7a}$$

$$\hat{\boldsymbol{y}} = G_y\boldsymbol{u} + H_y\hat{\boldsymbol{\eta}} \tag{7b}$$

If one now defines $\tilde{\boldsymbol{\eta}} := \hat{\boldsymbol{\eta}} - \boldsymbol{\eta}$, and given that $\boldsymbol{\eta}$ is assumed constant, from Eqs. (7a) and (7b), one has

$$\dot{\tilde{\boldsymbol{\eta}}} = \dot{\hat{\boldsymbol{\eta}}} = -K_0(\hat{\boldsymbol{y}} - \boldsymbol{y}) = -K_0H_y\tilde{\boldsymbol{\eta}} \tag{7c}$$

Inasmuch as, in practice, H_y is nonsingular [otherwise, as can be seen from Eq. (7b), the EDPs will not have independent effects on the measured outputs], one can always find $K_0 \in \mathbb{R}^{5\times5}$ such that

$$K_0H_y = \Lambda = \operatorname{diag}(\lambda_1, \lambda_2, \ldots, \lambda_5) \Rightarrow K_0 = \Lambda H_y^{-1} \tag{8}$$

where $\lambda_1, \lambda_2, \ldots, \lambda_5$ is a set of real negative constants selected to satisfy a compromise between convergence speed and noise rejection. The advantages of this method with respect to the KF given by Eqs. (4–6), concern its implementation, design, and tuning. They can be summarized as follows. As opposed to the KF, the tuning parameters are directly the (inverse of the) time constants of each of the estimation errors. The convergence speed of each of the estimates can therefore be adjusted individually and easily made independent of the power setting (or local model dynamics). Also, with Eq. (8), K_0 can be updated on-line using the current H_y that [together with G_y in Eq. (7b)] is available at any time for the optimization model. This avoids having to store and to select in-flight the matrices A, B, C, D, L, M, and K, thus reducing the complexity of the overall algorithm. Since the model used for estimation is the same as the model used for optimization, any possible inconsistency between both models is eliminated. The estimator's equations are simpler, and its dimension has been reduced from 8 to 5.

Comparison Between the SSMLO and the KF Approaches

Flight Conditions

The data were collected during a cruise steady-state flight test of the NASA Dryden F-15 test bed aircraft at 30,000-ft altitude, Mach 0.91, and 60-deg power lever angle, with the PSC algorithm in the minimum fuel mode.[2] The same input and output measurements are used for the KF and the SSMLO. The measured inputs and outputs are sampled at 8 Hz. EDPs normalization factors are shown in Table 1.

Results

An observer's settling time of 20 s was considered adequate for the application. Accordingly, the following set of eigenvalues was selected:

$$\lambda_1 = \lambda_3 = \lambda_4 = \lambda_5 = -0.3, \qquad \lambda_2 = -0.2 \tag{9}$$

An originally $\lambda_2 = -0.3$ value was modified a posteriori in order to improve the noise rejection capability of the estimator.

In Fig. 1, the EDPs estimated using the KF (Fig. 1a) are compared with those obtained with the SSMLO (Fig. 1b) using the same data.

The initial EDPs estimated values are assumed zeros for both estimators. As expected, both estimators converge to the same asymptotic values. The settling times of the SSMLOs estimates are in plain correspondence with the specified λ_i

Table 1 Factors that normalize EDPs

Component	Normalization factor
DEHPT	1%
DELPT	1%
DWHPC	60 lb/s
DWFAN	255 lb/s
AAHT	60 lb/s

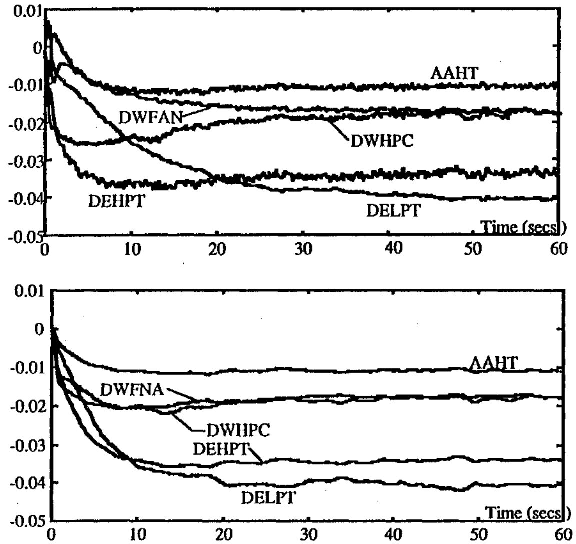

Fig. 1 Normalized estimated EDP: a) KF approach and b) SSMLO approach.

(four to five times the corresponding time constants: $1/\lambda_i$). For the KF, the settling times range from 6 to 8 s for DEHPT or AAHT, to approximately 35 s for DELPT. Note that there is a high-frequency residual noise with the KF. This is a consequence of its larger bandwidth associated with its fast modes.

Conclusions

The Kalman filter approach for the estimation process of PSC presents some practical inconveniences from the viewpoint of the analysis, implementation, tuning, and design. Most of these difficulties can be easily overcome if a simpler Luenberger-type observer is applied directly to the same steady-state model used for the optimization. With the Kalman filter approach, two independent sets of local linear models need to be stored in memory, whereas with the proposed technique the estimation and optimization processes share the same piecewise linear model. Thus, no extra on-line model switching is required, less computer memory is needed, and the identity between the local optimization model and the local estimation model is guaranteed at any moment. Furthermore, the convergence speed of each of the estimates can be adjusted individually and easily made independent of the power setting. Furthermore, the tuning procedure is straightforward. The tests with flight data from an F-15 propulsion system show that the neglected engine's dynamics do not have any noticeable effects on the estimates, and that similar or better noise rejection and convergence speed can be obtained.

References

[1]Luppold, R. H., Gallops, G., Kerr, L., and Roman, J. R., "Estimating In-Flight Engine Performance Variations Using Kalman Filter Concepts," AIAA Paper 89-2584, July 1989.

[2]Gilyard, G. B., and Orme, J. S., "Subsonic Flight Test Evaluation of a Performance Seeking Control Algorithm on an F-15 Airplane," AIAA Paper 92-3743, July 1992; also NASA TM-4400, Aug. 1992.

[3]Nobbs, S. G., Jacobs, S. W., and Donahue, D. J., "Development of the Full-Envelope Performance Seeking Control Algorithm," AIAA Paper 92-3748, July 1992.

[4]Orme, J. S., and Gilyard, G. B., "Subsonic Flight Test Evaluation of a Propulsion System Parameter Estimation Process for the F100 Engine," AIAA Paper 92-3745, July 1992; also NASA TM-4426, Nov. 1992.

[5]España, M. D., and Gilyard, G. B., "On the Estimation Algorithm of the Performance Seeking Controller for Turbofan Engines," NASA TM-4551, Nov. 1993.

[6]Kalman, R. E., and Bucy, R. S., "New Results in Linear Filtering and Prediction Theory," *Journal of Basic Engineering, Transactions of the American Society of Mechanical Engineers*, Series D, No. 3, 1961, pp. 95–108.

[7]Kailath, T., *Lectures on Wiener and Kalman Filtering*, CISM Courses and Lectures No. 140, International Centre for Mechanical Sciences, Springer-Verlag Wien, New York, 1981.